

# Roles of Aqueous Extract of Marigold on Arsenic-Induced Oxidative Damage in Pancreatic Islet $\beta$ -Cells

Zongqin Mei<sup>1\*</sup> , Jiao Dai<sup>2\*</sup> , Guofen Liu<sup>1</sup> , Zuoshun He<sup>1</sup> , Shiyun Gu<sup>1#</sup> 

<sup>1</sup>Institute of Preventive Medicine, School of Public Health, Dali University, Dali, China

<sup>2</sup>Experimental Training Teaching Management Office, Qujing Medical College, Qujing, China

Email: mzqin176323@163.com, qjzdaijoy@163.com, guofen207@163.com, hzs338@163.com, #ygsy727@163.com

**How to cite this paper:** Mei, Z.Q., Dai, J., Liu, G.F., He, Z.S. and Gu, S.Y. (2024) Roles of Aqueous Extract of Marigold on Arsenic-Induced Oxidative Damage in Pancreatic Islet  $\beta$ -Cells. *Journal of Biosciences and Medicines*, 12, 19-34.  
<https://doi.org/10.4236/jbm.2024.125003>

**Received:** March 3, 2024

**Accepted:** May 5, 2024

**Published:** May 8, 2024

Copyright © 2024 by author(s) and Scientific Research Publishing Inc.  
This work is licensed under the Creative Commons Attribution International License (CC BY 4.0).  
<http://creativecommons.org/licenses/by/4.0/>



Open Access

## Abstract

Roles of Marigold extracts (ME) on arsenic trioxide (ATO)-induced oxidative damage to pancreatic  $\beta$ -cells need to be further elucidated. In this study, NIT-1 cells were treated with different concentrations of and/or ATO, following by the cell viability was detected by CCK8 assay. Then, intracellular reactive oxygen species (ROS) levels, lipid peroxide (MDA) contents and superoxide dismutase (SOD) activity were measured with a fluorescence probe method and colorimetric assay, respectively. The apoptosis rate and morphology was detected and observed with hoechst 33,258 staining assay. The mRNA levels and protein expressions of nuclear factor E2-related factor 2 (Nrf2) and heme oxygenase-1 (HO-1) were measured by real-time fluorescence quantitative polymerase chain reaction and protein immunoblotting assay, respectively. Our results indicated that Co-treatment with ME and ATO exacerbated the cell viability decreasing reduced by ATO, while the addition of ME after ATO treatment effectively promote the recovery of ATO reduced survival rates. The ATO group increased apoptosis ( $P < 0.05$ ), while the ATO + ME-treated group alleviated apoptosis caused by ATO ( $P < 0.05$ ); ROS content was 1.49 and 1.26 times higher in the ATO and ATO + ME groups, respectively, compared with the control group; SOD activity in the ATO group ( $69.66 \pm 1.97$  U/mg Protein) was significantly lower than that in the SOD activity in the ATO group ( $69.66 \pm 1.97$  U/mg Protein) was significantly lower than that in the control group ( $85.18 \pm 4.57$  U/mg Protein) and the ATO + ME group ( $76.82 \pm 2.30$  U/mg Protein); MDA content in the ATO group ( $3.78 \pm 0.22$  nmol/mg protein) was significantly higher than that in the control group

\*The authors contribute equally to the article.

#Corresponding author.

( $2.71 \pm 0.21$  nmol/mg protein) and the ATO + ME group ( $3.13 \pm 0.19$  nmol/mg protein); the mRNA levels of HO-1 and Nrf2 were elevated in the ATO group and ATO + ME-treated group compared with the control group, and the trends of protein expression levels of HO-1 and Nrf2 were consistent with the trends of mRNA levels. The results of this study suggest that aqueous extracts of Marigold may be involved in antagonizing arsenic-induced oxidative damage in pancreatic  $\beta$ -cells by modulating the activation of the Nrf2 signaling pathway.

## Keywords

Arsenic Trioxide, Marigold Extracts, Nuclear Factor E2-Related Factor 2, Oxidative Damage

---

## 1. Introduction

As a common environmental heavy metal contaminant, arsenic is widely found in the natural environment [1]. Epidemiological evidence has suggested that chronic arsenic exposure increased the risk of developing type 2 diabetes [2] [3], underlying which the mechanisms related to the arsenic-induced impairment of pancreatic  $\beta$ -cell function through increasing the production of reactive oxygen species (ROS) and disrupting redox homeostasis [4] [5] [6]. Marigold is a genus of plants in the daisy family Marigold, which contains antioxidant compounds such as luteolin, phenolics and so forth [7]. Previous studies have reported that the Marigolds extracts (ME) was able to remove excess ROS from cells to prevent the oxidation of intracellular biomolecules by oxygen free radicals [8] [9]. In addition, ME also has been demonstrated to reduce oxidative damage in kidneys caused by anti-tumor medicines [10] [11]. However, does ME antagonize arsenic-induced oxidative damage to pancreatic islet beta cells? What are the mechanisms involved? No research has been reported so far.

Nuclear factor erythroid 2-related factor 2 (Nrf2) is an important transcription factor that regulates the cellular antioxidant response [12]. Studies have shown that Nrf2 mediates the activation of antioxidant signaling pathways and plays essential roles in the defense mechanism of pancreatic  $\beta$ -cells against arsenic toxicity. Specifically, Nrf2 knockout pancreatic  $\beta$ -cells are more sensitive to the toxicity induced by arsenic [13] [14]. In addition, Marigold essential oil against N-methyl-N'-nitro-N-nitrosoguanidine (MNNG)-induced gastric cancer tumorigenesis through attenuating the oxidative stress, apoptotic response and inflammatory response through Nrf2/HO-1 and NF- $\kappa$ B signaling pathways [15]. Also, ME reduced colitis severity and ROS levels by inhibiting inflammatory cytokine secretion [16]. In a word, present studies have suggested that ME may have an activating effect on Nrf2-mediated antioxidant signaling pathway, so can the ME affect the arsenic-induced oxidative damage in pancreatic  $\beta$ -cells by influencing the level of Nrf2? There is no clarity yet.

In this study, cell viability, reactive oxygen species (ROS), superoxide dismutase (SOD), malondialdehyde (MDA), apoptosis were used to assess the reversal effects of ME on ATO-induced cell damage. Further, mRNA levels and protein expressions of heme oxygenase-1 (HO-1) and Nrf2 were also detected to clarify whether the Nrf2 signaling pathway is involved in ME antagonizing arsenic induced oxidative stress. Our experimental results will provide scientific basis for the application of ME in the prevention and treatment of arsenic toxicity.

## 2. Methods

### 2.1. Extraction of Aqueous Extract of Marigold

Putting the dried flowers of Marigold into the Chinese medicine crusher for 1 min, and pass the obtained powder of Marigold flowers through a standard mesh sieve of 60 mesh to obtain 60 mesh Marigold powder. Weighing 10.0 g of 60 mesh Marigold powder and 200 mL of distilled water, mix thoroughly, maintaining for 2 h at 100°C in a water bath, extracting three times, combining the three filtrates and filter. The filtrate was spin-distilled at 45°C under RE2000 Series Rotary Evaporator (Shanghai Yarong Biochemical Instrument Factory), until about 1 mL of spin-distilled liquid was in the spin-distillation bottle. The liquid was transferred to a Petri dish with a pasteurized pipette, wrapped in cling film and frozen in Scientz-ND Series Vacuum Freeze Dryer (Ningbo Xinzhi Biotechnology Co., Ltd.) at -20°C for 7 h, then put into a freeze-dryer for 12 h to obtain a freeze-dried powder of water-soluble ingredients of Marigold, which was stored at 4°C for alternate use.

Weighing 100 mg of lyophilized powder of Marigold water-soluble ingredients, dissolve in 10 mL of distilled water and prepare 10<sup>4</sup> mg/L of application solution, store at 4°C for alternate use.

### 2.2. Cell Culture

A pancreatic beta-cell line established from transgenic mice, named NIT-1 cells, purchased from Guangzhou Jennio Biotech Co., Ltd. NIT-1 cells were cultured in 1640 medium (Life Technologies/Gibco, Grand Island, NY, USA) containing 10% fetal bovine serum (Biopike Biotechnology Co., Ltd., Beijing, China) and 100 unit/mL penicillin and 100 mg/L streptomycin in a cell incubator at 37°C and saturated humidity with 5% CO<sub>2</sub>. Cells were passaged once when they had grown to cover about 90% of the wall area of the culture flask.

### 2.3. Determination of Cell Viability

The cell viability was detected with a CCK-8 kit (Nanjing Jiancheng Institute of Biological Engineering). NIT-1 cells were seeded into in 96-well plates at density of 1 × 10<sup>5</sup> cells/well, and cultured for 24 h at 37°C in 5% CO<sub>2</sub> incubator. Cells were treated with different concentrations (0, 0.4, 0.8, 1.6, 3.2, 6.4, 12.8 mg/L) of ATO (Arsenic trioxide (As<sub>2</sub>O<sub>3</sub>, Beijing Tanmo Quality Control Technology Co., Ltd.) and different concentrations (0, 40, 80, 160, 320, 640, 1280 mg/L) of ME for

24 h. Then, the toxic liquid was discarded and the cells were incubated in a medium mixed with 10  $\mu$ L CCK8 solution and 90  $\mu$ L 1640 at 37°C, 5% CO<sub>2</sub>, and 90% humidity for 4 h. The absorbance was subsequently measured at 450 nm with a multifunctional fluorescent plate instrument (SP-Max3500FL, Flash Biotechnology Co., Ltd., Shanghai, China). Cell survival rate was calculated according to cell survival rate = [(experimental hole – blank hole)/(negative control hole – blank hole)]  $\times$  100%.

#### **2.4. Hoechst 33,258 Staining**

Hoechst 33,258 staining (Beyotime Institute of Biotechnology, Jiangsu, China) was used to evaluate the morphological changes of the cells undergoing apoptosis and detect apoptosis rate. NIT-1 cells were seeded into in 6-well plates at  $1 \times 10^6$  cells/well, overnight cultured and after the designed treatment, cells were fixed and stained with Hoechst 33,258 solution according to the manufacturer instructions. Cells were then stimulated by ultraviolet light under a fluorescence microscope and photographed in a random 3 - 5 field of view under the microscope. Apoptotic cells were defined by the condensation of nuclear chromatin, fragmentation, or margination to the nuclear membrane. We counted 200 cells under the microscope and recorded the number of apoptotic cells. Apoptosis rate (%) was equal to apoptotic cell number/200  $\times$  100%.

#### **2.5. Measurement of Reactive Oxygen Species (ROS) Generation**

The intracellular ROS was detected using a reactive oxygen detection kit (Shanghai Beyotime Biotechnology Co., Ltd). According to the manufacturer's instruction, NIT-1 Cells were seeded into in 6-well plates at  $1 \times 10^6$  cells/well, overnight cultured and after the ATO and ME treatment, adding 1000  $\mu$ L of culture medium containing DCFH-DA probe with concentration of 10  $\mu$ mol/L to each well and incubate for 20 min in the dark at 37°C. Afterward, cells were washed twice with cold PBS followed by observing and photographing in a random 3 - 5 field of view under a fluorescence microscope (Olympus Corp, Tokyo, Japan). Average ROS fluorescence intensity = total optical density/cell area.

#### **2.6. Detection of Superoxide Dismutase (SOD) Activity**

Total SOD activity was determined with a SOD assay Kit (Shanghai Beyotime Biotechnology Co., Ltd). NIT-1 cells were seeded into in 6-well plates at  $1 \times 10^6$  cells/well, overnight cultures, followed by the prescribed treatment, sample loading, incubation and detection were carried out according to the steps in the manufacturer. The activities of SOD were standardized by protein concentrations, which were determined by the BCA Protein Assay Kit (Shanghai Beyotime Biotechnology Co., Ltd). The total SOD activity was normalized by the protein concentrations.

#### **2.7. Malondialdehyde (MDA) Content Assay**

MDA was tested with MDA assay Kit (Shanghai Beyotime Biotechnology Co.,

Ltd). NIT-1 Cells were seeded into in 6-well plates at  $1 \times 10^6$  cells/well, after an overnight culture and the prescribed course of therapy, cells were harvested and lysed in lysis bufer (Shanghai Beyotime Biotechnology Co., Ltd) for 10 min at 4°C. Afterward, cell suspension was centrifuged at 13,000 rpm for 10 min and cell supernatants were collected for detecting the content of MDA. Following the manufacturer's instructions for sample loading, incubation, and detection, the MDA content has been standardized by protein concentrations, which were determined by the BCA Protein Assay Kit (Shanghai Beyotime Biotechnology Co., Ltd). The content of MDA was normalized by the protein concentrations.

## 2.8. Fluorescence Quantitative Real-Time Polymerase Chain Reaction (qPCR)

Total RNAs were isolated using a total RNA extraction kit (Tiangen Biotech, Beijing Co., Ltd, China). The quality and concentration of total RNAs were evaluated by ultra-micro ultraviolet-visible spectrophotometer (Hangzhou Suizhen Biotechnology Co., Ltd). For specific RNA sample, ratio of  $A_{260}/A_{230}$  and  $A_{260}/A_{280}$  both between 1.8 and 2.2 has been considered qualified and can be used for subsequent experiments. Qualified RNA sample was then reversed transcription to obtain the DNA sample, closely followed by 200 ng cDNA template for PCR amplification. The reaction conditions were as follow: 95°C for 15 min 1 cycle (pre-denaturation), 95°C for 10 s 40 cycles (denaturation), 60°C for 32 s 40 cycles (annealing/extension). All the primers for mRNAs were synthesized by Shanghai Generay biological engineering Co., Ltd. (Shanghai, China), and the sequences of each primer were listed in **Table 1**. The *glyceraldehyde-3-phosphate dehydrogenase gene* (GAPDH) was used as the internal control and levels of mRNA were calculated by the equation  $2^{-\Delta\Delta Ct}$  ( $\Delta Ct = Ct_{mRNA} - Ct_{GAPDH}$ ,  $\Delta\Delta Ct = \Delta Ct_{Treatment} - \Delta Ct_{Control}$ ).

## 2.9. Western Blot Analysis

The protein expression of apoptosis-related proteins was detected by Western Blot analysis, the protein concentrations were determined by the BCA Protein Assay Kit (Shanghai Beyotime Biotechnology Co., Ltd). Subsequently, equal

**Table 1.** Real-time PCR primer sequences.

Primer names	Primer sequences
<i>GAPDH</i>	F-AGGTCGGTGTGAACGGATTTG
	R-TGTAGACCATGTAGTTGAGGTCA
<i>Nrf2</i>	F-TCAGCGACGGAAAGAGTATGA
	R-CCACTGGTTTCTGACTGGATGT
<i>HO-1</i>	F-AAGACTGCGTTCCTGCTCAAC
	R-AAAGCCCTACAGCAACTGTCTG

amounts of protein (60 µg) separated by 12% sodium dodecyl sulfate polyacrylamide gel electrophoresis (SDS-PAGE) and transferred onto polyvinylidene difluoride (PVDF) membranes (Millipore, MA, USA). The membrane was then blocked with 5% non-fat milk for 2 h and incubated with primary antibodies against HO-1 and Nrf2 (1:500) (Beijing solarbio Technology Co., Ltd.) and GAPDH (1:1000) antibody (Shanghai Jereh Bioengineering Co., Ltd.) overnight at 4°C. The membranes were further incubated with horseradish-peroxidase-conjugated secondary antibodies (ZSGB Bio, Beijing, China, 1:6000) at room temperature for 1 h. The immuno-reactivity zone was observed with enhanced chemiluminescence reagent (Millipore, temecula, CA) and displayed with JS-M6 chemiluminescence imaging system. Image J software was utilized to analyze the average optical density of protein bands and GAPDH was used as the internal reference to correct the grayscale value of the target band protein. The relative expression level of the protein was equal to the grayscale value of the measured band/the grayscale value of the internal reference. The protein expression of the control group was used to correct the results.

### 2.10. Statistical Analysis

All experiments were repeated three times independently, and the results were presented as mean ± standard deviation (SD). Differences among groups were performed by using one-way analysis of variance (ANOVA) analysis. Student-NewmanKeuls (SNK) test was used to compare the means of two independent groups. Non-parametric Kruskal-Wallis test was used when the original data were under variance heterogeneity. Statistical significance was set as  $P < 0.05$ . All statistical analysis were performed using the Statistical Program for Social Sciences (SPSS), version 20.0 (SPSS, Inc., Chicago, IL, USA).

## 3. Results

### 3.1. Antagonistic Effects of ME on ATO-Induced the Cell Viability in NIT-1 Cells

As shown in **Figure 1(a)**, after treatment with 0.4 mg/L ATO, the cell viability decreased in a dose-dependent way. In **Figure 1(b)** ME at 40 mg/L and 80 mg/L increased cell viability, from 100% to 105.12% and 111.64%, respectively, and the concentrations of ME above 80 mg/L decreased cell viability, as well as in a dose-dependent way. Notably, as shown in **Figure 2(a)** and **Figure 2(b)**, combination of ME and ATO synergistically reduced the cell viability of NIT-1 cells to 38.60%, showing lower cell survival rate than those of single ME or ATO treated groups. These results indicate that combination of ME with ATO is capable to increase the sensitivity of ATO for killing NIT-1 cells. However, when ME treatment was given 24 h after ATO treatment, the cell survival rate was higher than that of the ATO group, changing from 67.68% to 78.20%. These results indicate that ME was able to reverse the killing effect of ATO on NIT-1 cells. This treatment was used in subsequent experiments.

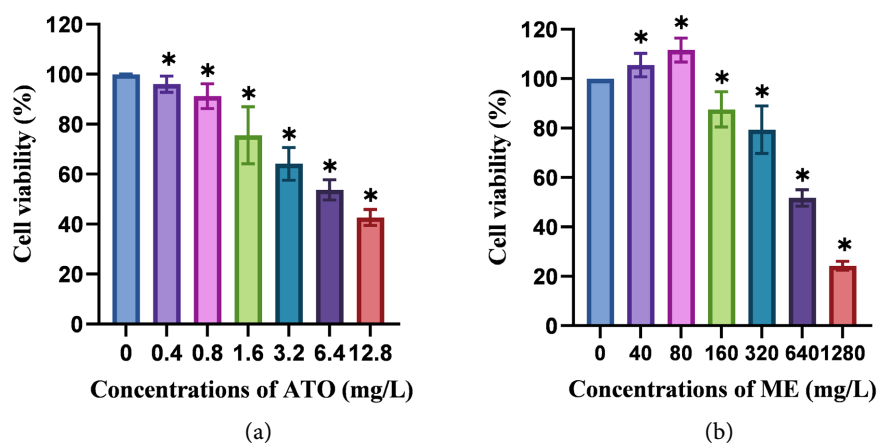


**Figure 1.** Effect of ATO and ME on cell viability. (a) Effect of different concentrations of ATO on cell viability; (b) Effect of different concentrations of ME on cell viability. \*: statistically significant difference with control group,  $P < 0.05$ .

### 3.2. Antagonistic Effects of ME on ATO-induced Cell Apoptosis in NIT-1 Cells

In the Hoechst 33,258 fluorescent staining assay, the nuclei of control cells and ME-treated cells showed an oval round shape with homogenous intensity and were very lightly stained, whereas cells treated with ATO were found in a condensed and/or fragmented shape with irregularity and bright staining (Figure 2(c)). These apoptotic morphological changes showed greater difference in cells simultaneously treated with higher doses of ATO. As shown in Figure 2(d) and Figure 2(c), there was no significant difference between the ME group and the control group in apoptotic morphological changes, and there was no significant difference in the apoptotic rate between the two groups ( $p > 0.05$ ). After ME treatment, the morphological changes of apoptosis induced by ATO decreased significantly, and the apoptosis rate decreased. The rate of apoptosis in the ATO group was 2.88 times of that in the control group, whereas, after ME treatment, the rate of apoptosis in the ME + ATO group was 2.11 times of the control group. These results indicate that ME treatment can reverse ATO-induced apoptosis.

### 3.3. Antagonistic Effects of ME on ATO-induced Oxidative Stress in NIT-1 Cells

As shown in Figure 3(a), ATO exposure led to the accumulation of reactive oxygen species, but ME treatment facilitated the ATO-induced removal of ROS. Fluorescence quantitative results further showed that treatment with ATO and ATO + ME led to an 49% and 29% increase on ROS production in comparison to control cells (Figure 3(b)).

In order to comprehensively evaluate the degree of oxidative damage, we further detected the SOD activities and MDA contents in ME-treated, ATO-treated and ATO + ME-treated NIT-1 cells. The results demonstrated that SOD activity respectively were 95.98 U/mg protein, 69.66 U/mg protein, or 76.82 U/mg



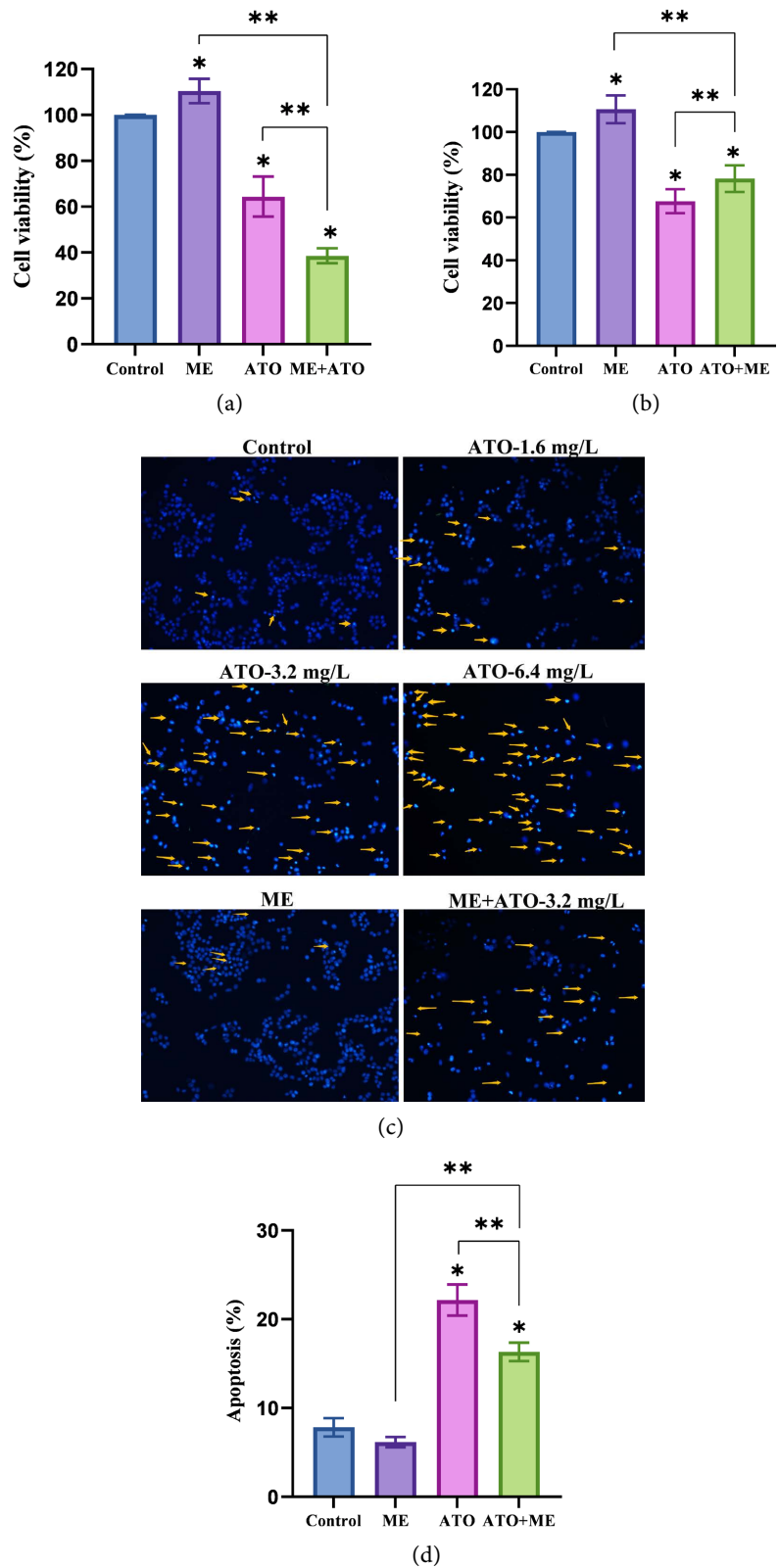


**Figure 2.** Effect of ME on ATO-induced cell viability and apoptosis. (a) ATO and ME co-treatment; (b) The ATO is treated 24 h prior to joining the ME; (c) Apoptosis; (d) Apoptosis rate. \*: statistically significant difference between representative and control groups,  $P < 0.05$ . \*\*: statistically significant difference between the two groups,  $P < 0.05$ .



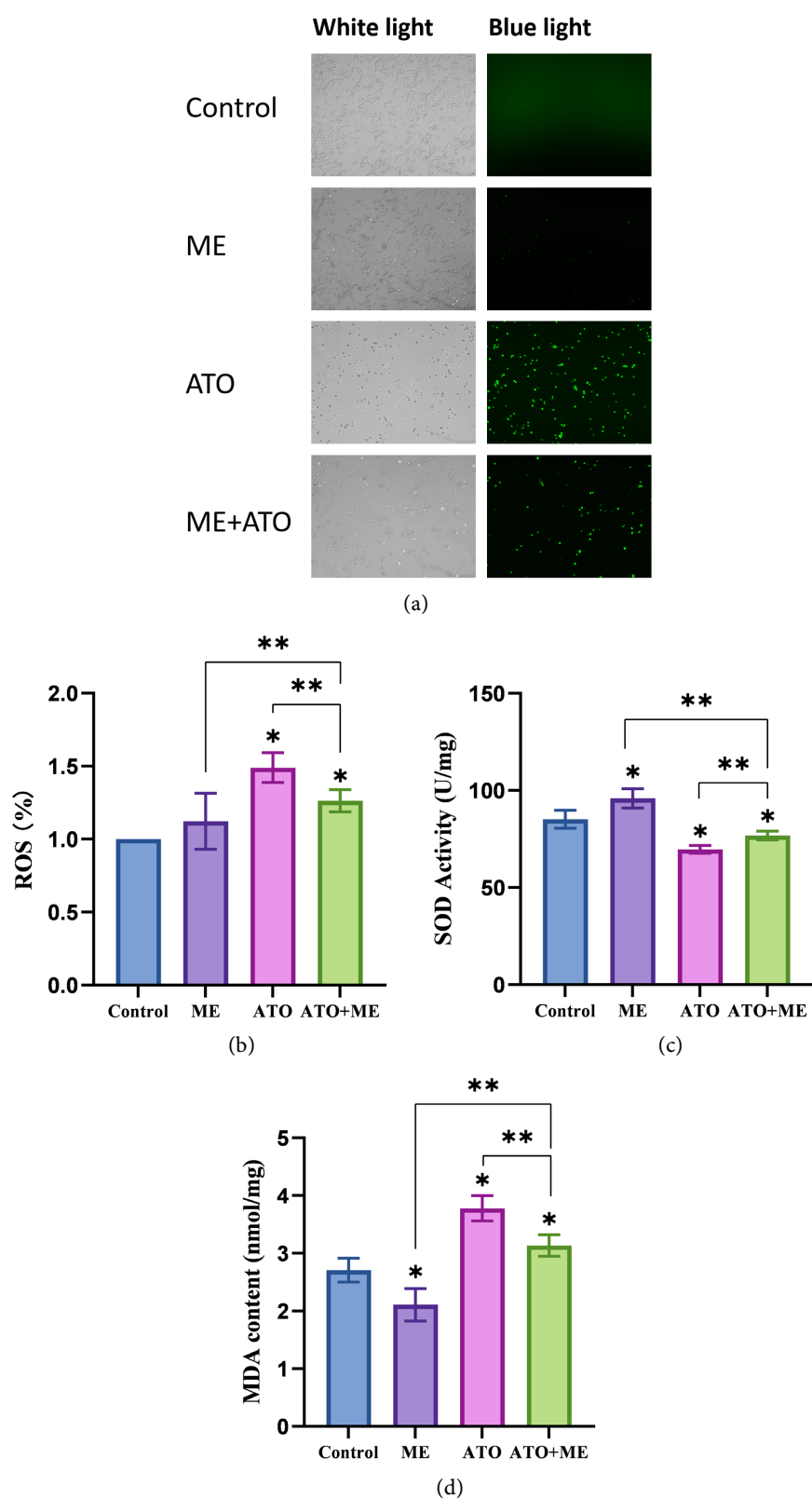


**Figure 3.** Antagonistic effects of ME on ATO-induced oxidative stress. (a) Comparison graph of ROS; (b) Percentage of ROS; (c) SOD level; (d) MDA level. \*: statistically significant difference compared to the control group,  $P < 0.05$ . \*\*: statistically significant difference between two groups,  $P < 0.05$ .

protein in NIT-1 cells which was exposed to ME, ATO and ATO + ME. SOD activity was lower in the ATO and ATO + ME groups than that in the control group (85.18 U/mg protein), and it was higher than that in the ATO + ME group when compared to the ATO group (Figure 3(c)). By contrast, MDA contents were  $3.78 \pm 0.22$  nmol/mg protein and  $3.13 \pm 0.19$  nmol/mg protein in ATO and ME + ATO treatment cells (Figure 2(c)). MDA levels were higher in the ATO and ATO + ME groups than that in the control group ( $2.71 \pm 0.21$  nmol/mg protein), while lower in the ATO + ME group in comparison to the ATO group.

### 3.4. Antagonistic Effects of ME on ATO-Induced HO-1 and Nrf2 mRNA Levels

An increase in Nrf2 and HO-1 mRNA levels was clearly observed in the ATO group, while Nrf2 and HO-1 mRNA levels were lower in the ME + ATO group compared to the ATO group, as shown in Figure 4. For ATO group and ME + ATO group, the HO-1 mRNA levels were 21.65-fold and 8.17-fold of untreated group respectively ( $P < 0.05$ ), the Nrf2 mRNA levels were 3.05-fold and 1.42-fold of untreated group respectively ( $P < 0.05$ ). Incidentally, both Nrf2 and HO-1 mRNA levels of the ME group were slightly lower than in the untreated group.

### 3.5. Antagonistic Effects of ME on ATO-induced HO-1 and Nrf2 Protein Levels

As illustrated in Figure 5, protein expressions of Nrf2 and HO-1 have similar tendencies to the changes of mRNA levels. In detail, the protein of Nrf2 in control group, ME group, ATO group and ATO + ME group was 1-fold, 1.01-fold, 1.84-fold and 1.39-fold, respectively. Also, HO-1 was increased after treatment with ATO and ATO + ME in comparison to control group (1.84-fold, 1.39-fold).

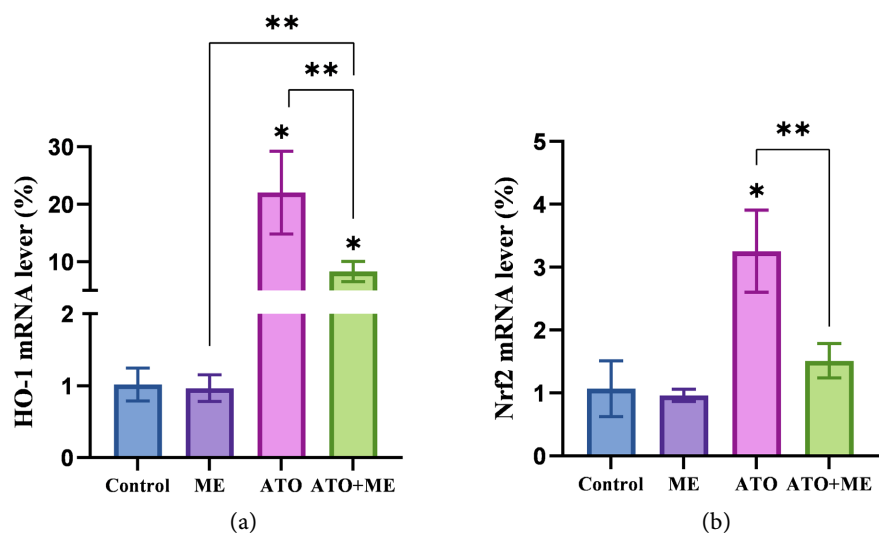


**Figure 4.** Antagonistic effects of ME on ATO-induced HO-1 and Nrf2 mRNA levels (a) HO-1 mRNA expression level; (b) Nrf2 mRNA expression level. \*: statistically significant difference compared with the control group,  $P < 0.05$ ; \*\*: statistically significant difference between the two groups,  $P < 0.05$ .

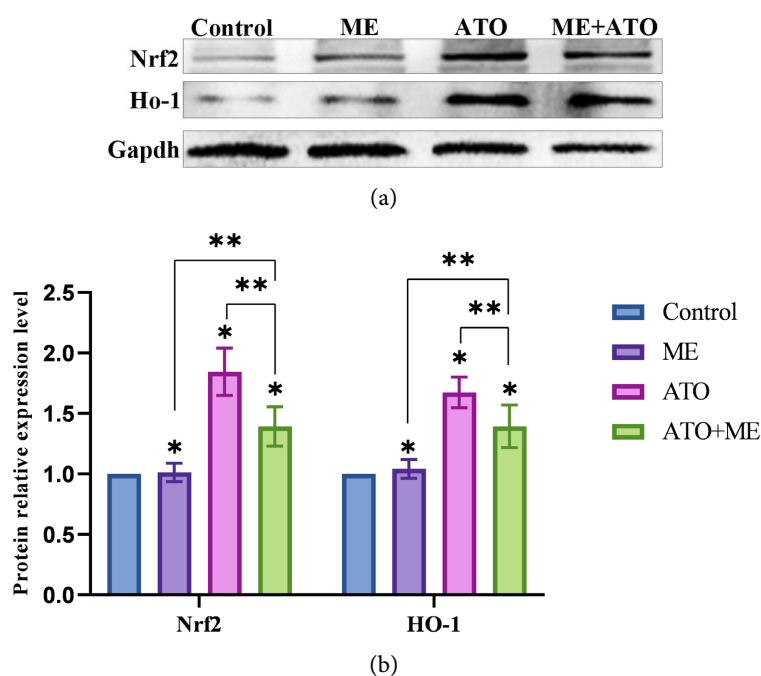


**Figure 5.** Antagonistic effects of ME on ATO-induced HO-1 and Nrf2 protein levels. (a) Immunoblotted protein bands; (b) Relative protein expression levels. \*: statistically significant difference compared with the control group,  $P < 0.05$ . \*\*: statistically significant difference between the two groups,  $P < 0.05$ .

#### 4. Discussion

Arsenic-induced cytotoxicity is a fundamental cause of the development of arsenic-related diseases [17], and long-term exposure to arsenic can increase the risk of type 2 diabetes. The mechanism involved may be related to the functional impairment of pancreatic  $\beta$  cells induced by arsenic [4] [5]. Previous studies have shown that arsenic caused liver injury by inducing oxidative stress in normal liver cells (MIHA cells) [18]. Exists a comparable mechanism for islet cells? Arsenic exposure in animal models was associated with dysfunction in a variety of cell types and tissues, including liver and islets, according to Beck *et al.* Moreover, oxidative stress is the most detrimental consequence of arsenic exposure on islet cells *in vitro* and/or *in vivo*, resulting in islet dysfunction [19]. In accordance with this conclusion, our results also suggest that arsenic exposure induces oxidative damage to NIT-1 cells (Figure 3), suggesting that arsenic may induce type 2-diabetes by damaging islet cells.

Due to its pharmacological properties, the traditional Chinese herb marigold is widely used for the prevention and treatment of various diseases [20]. Recent research has revealed that marigold contains a high concentration of nutrients, including luteolin and phenolics [8] [9] [21]. Marigold extracts have potent antioxidant activity, which is primarily attributable to the presence of polyphenolic active substances in Marigold [9], which is one of the plant polyphenols and a complex phenolic secondary metabolite found primarily in the leaves, fruits, roots, and bark of plants [21]. Plant polyphenols have a long history of research

and have been shown to have powerful antioxidant effects, anti-tumor, anti-bacterial, anti-atherosclerosis, and other physiological functions; they are considered the “health guards” of nature and humanity [22]. However, it has not been determined whether polyphenol-rich Marigold can counteract the oxidative damage induced by arsenic. Therefore, we treated NIT-1 cells with ME and ATO to determine the antagonistic effect of Marigold on arsenic-induced oxidative damage.

In this study, ME at low concentrations (80 mg/L) promoted the viability of NIT-1 cells; however, above 80 mg/L, a dose-dependent decrease in cell viability was observed, indicating that ME at high concentrations still had some deleterious effects on cells. Co-treatment with 80 mg/L ME and 3.2 mg/L ATO resulted in a greater NIT-1 cell death than ATO alone. However, the addition of ME after 24 h of ATO treatment effectively reversed the cell mortality induced by ATO, indicating that ME could be used as a therapeutic agent for arsenic toxicity in clinical practice, although caution should be exercised when determining the dose.

It is well known that Nrf2 is an important transcription factor regulating cell redox balance [12] [23], and HO-1 is one of the antioxidant enzymes activated by Nrf2 [24] [25]. Studies have shown that during ROS formation, the activation of the Nrf2 signaling pathway is of great significance for maintaining pancreatic  $\beta$  cell function [26]. In addition, *Zheng et al.* discovered that the intestinal metabolite of ellagitannin (a plant polyphenol), urea B (UB), promoted nuclear translocation of Nrf2 during Ischemia/reperfusion injury, and that Nrf2 gene silencing diminished the protective effect of UB on superoxide production and apoptotic cell death [27]. Tea polyphenols consistently protect endogenous dopamine neurons by inhibiting endogenous dopamine oxidation, scavenging ROS, and modulating the Nrf2-Keap1 pathway, according to *Zhou et al.* [28]. These studies indicate that plant polyphenols can restore oxidative damage via the Nrf2 signalling pathway. Previous reports have confirmed that arsenic exposure can activate the Nrf2 signaling pathway [29] [30]. So, for Marigold, which is also rich in plant polyphenols, does the Nrf2 signalling pathway play a specific function in promoting recovery from arsenic-induced oxidative damage? The mRNA and protein expression levels of Nrf2 and HO-1 substantially increased in NIT-1 cells following ATO treatment, suggesting that exposure to arsenic activated the Nrf2 signalling pathway. In contrast, after Marigold treatment, the mRNA and protein expression levels of Nrf2 and HO-1 decreased. Marigold aqueous extract was hypothesised to have an activating effect on the Nrf2 signalling pathway. In conclusion, the mRNA and protein expression levels of Nrf2 and HO-1 decreased following Marigold treatment, and the arsenic-induced oxidative damage in pancreatic-cells was ameliorated, indicating that Marigold aqueous extract may inhibit the arsenic-induced oxidative damage in NIT-1 cells by regulating the Nrf2 signalling pathway. Our experimental results showed that Marigold extract has certain antioxidant properties, and can antagonize the cell

damage caused by arsenic induced oxidative stress of NIT-1, and arsenic treatment will induce oxidative damage of islet cells, which may lead to type 2 diabetes. The appearance of marigold water extract alleviates the oxidative damage caused by arsenic treatment to a certain extent, and can be used as an easily available antioxidant to alleviate the oxidative stress damage caused by arsenic treatment in the future.

## 5. Conclusion

In summation, our results indicated that Marigold water extract could repair the arsenic-induced damage to islet cells. Further analysis revealed that the mRNA and protein levels of Nrf2 and HO-1 were lower in the ATO + ME group compared to the ME group. By regulating the Nrf2/HO-1 pathway, it is hypothesized that ME can effectively repair the oxidative damage caused to NIT-1 cells by ATO. This provides a novel concept for the future clinical treatment of acute arsenic toxicity.

## Funding

This research was supported by the Joint Special Fund for Basic Research in Chinese Medicine, Yunnan Provincial Science and Technology Department (No. 202101AZ070001-085) to Jiao Dai, and by the grants from the National Natural Science Foundation of China (No. 82060585; No. 82260631) to Shiyan Gu and Zuoshun He.

## Author Contributions

Zongqin Mei and Jiao Dai contributed to writing the article, checking the content and sorting out the literature. Guofen Liu contributed to reference collection, induction and verification. Zuoshun He and Shiyan Gu revised the manuscript. All authors are read and revised the published version of the manuscript.

## Data Availability

The data of this study will be made available from the corresponding author on reasonable request.

## Conflicts of Interest

The authors declare no conflicts of interest regarding the publication of this paper.

## References

- [1] El-Ghiaty, M.A. and El-Kadi, A. (2023) The Duality of Arsenic Metabolism: Impact on Human Health. *Annual Review of Pharmacology and Toxicology*, **63**, 341-358. <https://doi.org/10.1146/annurev-pharmtox-051921-020936>
- [2] Wu, M., Pang, C., Lu, S., Hostetter, T.H. and Hai, X. (2023) Type 2 Diabetes Affects Arsenic Metabolism via Transporters in Arsenic Trioxide Treated Acute Promyelo-

- cytic Leukemia Patients. *Environmental Toxicology and Pharmacology*, **100**, Article ID: 104142. <https://doi.org/10.1016/j.etap.2023.104142>
- [3] Zhang, Y., Zhou, M., Liang, R., Yu, L., Cheng, M., Wang, X., Wang, B. and Chen, W. (2023) Arsenic Exposure Incurs Hyperglycemia Mediated by Oxidative Damage in Urban Adult Population: A Prospective Cohort Study with Three Repeated Measures. *Environmental Research*, **229**, Article ID: 116009. <https://doi.org/10.1016/j.envres.2023.116009>
- [4] Shiek, S.S., Sajai, S.T. and Dsouza, H.S. (2023) Arsenic-Induced Toxicity and the Ameliorative Role of Antioxidants and Natural Compounds. *Journal of Biochemical and Molecular Toxicology*, **37**, e23281. <https://doi.org/10.1002/jbt.23281>
- [5] Todero, J.E., Koch-Laskowski, K., Shi, Q., Kanke, M., Hung, Y.H., Beck, R., Styblo, M. and Sethupathy, P. (2022) Candidate Master MicroRNA Regulator of Arsenic-Induced Pancreatic Beta Cell Impairment Revealed by Multi-Omics Analysis. *Archives of Toxicology*, **96**, 1685-1699. <https://doi.org/10.1007/s00204-022-03263-9>
- [6] Ozfidan-Konakci, C., Yildiztugay, E., Arikan, B., Alp-Turgut, F.N., Turan, M., Cavusoglu, H. and Sakalak, H. (2023) Responses of Individual and Combined Polystyrene and Polymethyl Methacrylate Nanoplastics on Hormonal Content, Fluorescence/Photochemistry of Chlorophylls and ROS Scavenging Capacity in Lemna Minor under Arsenic-Induced Oxidative Stress. *Free Radical Biology and Medicine*, **196**, 93-107. <https://doi.org/10.1016/j.freeradbiomed.2023.01.015>
- [7] Ji, S.M., Muthurasu, A. and Kim, H.Y. (2023) Marigold Flower-Shaped Metal-Organic Framework Supported Manganese Vanadium Oxide Electrocatalyst for Efficient Oxygen Evolution Reactions in an Alkaline Medium. *Chemistry*, **29**, e202300137. <https://doi.org/10.1002/chem.202300137>
- [8] Fatima, A., Farid, M., Asam, Z., Zubair, M., Farid, S., Abbas, M., Rizwan, M. and Ali, S. (2023) Efficacy of Marigold (*Tagetes erecta* L.) for the Treatment of Tannery and Surgical Industry Wastewater under Citric Acid Amendment: A Lab Scale Study. *Environmental Science and Pollution Research International*, **30**, 43403-43418. <https://doi.org/10.1007/s11356-023-25299-9>
- [9] Jadoon, S., Karim, S., Bin, A.M., Akram, M.R., Khan, A.K., Malik, A., Chen, C. and Murtaza, G. (2015) Anti-Aging Potential of Phytoextract Loaded-Pharmaceutical Creams for Human Skin Cell Longevity. *Oxidative Medicine and Cellular Longevity*, **2015**, Article ID: 709628. <https://doi.org/10.1155/2015/709628>
- [10] Gongadze, M., Machavariani, M., Enukidze, M., Gogia, N., Iobadze, M. and Chkhikvishvili, I. (2019) French Marigold (*Tagetes patula* L.) Flower Extract Protects Kidney Cells from Inflammation *in Vitro*. *Georgian Medical News*, No. 297, 154-157.
- [11] Casanova, A.G., Hernandez-Sanchez, M.T., Martinez-Salgado, C., Morales, A.I., Vicente-Vicente, L. and Lopez-Hernandez, F.J. (2020) A Meta-Analysis of Preclinical Studies Using Antioxidants for the Prevention of Cisplatin Nephrotoxicity: Implications for Clinical Application. *Critical Reviews in Toxicology*, **50**, 780-800. <https://doi.org/10.1080/10408444.2020.1837070>
- [12] Liu, D., Xu, G., Bai, C., Gu, Y., Wang, D. and Li, B. (2021) Differential Effects of Arsenic Species on Nrf2 and Bach1 Nuclear Localization in Cultured Hepatocytes. *Toxicology and Applied Pharmacology*, **413**, Article ID: 115404. <https://doi.org/10.1016/j.taap.2021.115404>
- [13] Yang, B., Fu, J., Zheng, H., Xue, P., Yarborough, K., Woods, C.G., Hou, Y., Zhang, Q., Andersen, M.E. and Pi, J. (2012) Deficiency in the Nuclear Factor E2-Related Factor 2 Renders Pancreatic Beta-Cells Vulnerable to Arsenic-Induced Cell Damage. *Toxicology and Applied Pharmacology*, **264**, 315-323. <https://doi.org/10.1016/j.taap.2012.09.012>

- [14] Chu, C., Gao, X., Li, X., Zhang, X., Ma, R., Jia, Y., Li, D., Wang, D. and Xu, F. (2020) Involvement of Estrogen Receptor-Alpha in the Activation of Nrf2-Antioxidative Signaling Pathways by Silibinin in Pancreatic Beta-Cells. *Biomolecules & Therapeutics (Seoul)*, **28**, 163-171. <https://doi.org/10.4062/biomolther.2019.071>
- [15] Cui, G., Wei, F., Wei, M., Xie, L., Lin, Z. and Feng, X. (2021) Modulatory Effect of *Tagetes erecta* Flowers Essential Oils via Nrf2/HO-1/NF-KappaB/P65 Axis Mediated Suppression of N-Methyl-N'nitro-N-Nitroguanidine (MNNG) Induced Gastric Cancer in Rats. *Molecular and Cellular Biochemistry*, **476**, 1541-1554. <https://doi.org/10.1007/s11010-020-04005-0>
- [16] Meurer, M.C., Mees, M., Mariano, L., Boeing, T., Somensi, L.B., Mariott, M., Da, S.R., Dos, S.A., Longo, B., Santos, F.T., Klein-Junior, L.C., De Souza, P., De Andrade, S.F. and Da, S.L. (2019) Hydroalcoholic Extract of *Tagetes erecta* L. Flowers, Rich in the Carotenoid Lutein, Attenuates Inflammatory Cytokine Secretion and Improves the Oxidative Stress in an Animal Model of Ulcerative Colitis. *Nutrition Research*, **66**, 95-106. <https://doi.org/10.1016/j.nutres.2019.03.005>
- [17] Kepp, O., Pan, H., Liu, P. and Kroemer, G. (2023) Arsenic Trioxide as an Inducer of Immunogenic Cell Death. *Oncoimmunology*, **12**, Article ID: 2174723. <https://doi.org/10.1080/2162402X.2023.2174723>
- [18] Wang, Q. and Zhang, A. (2023) Baicalein Alleviates Arsenic-Induced Oxidative Stress through Activation of the Keap1/Nrf2 Signalling Pathway in Normal Human Liver Cells. *Current Molecular Medicine*, **24**, 355-365. <https://doi.org/10.2174/1566524023666230320163238>
- [19] Beck, R., Styblo, M. and Sethupathy, P. (2017) Arsenic Exposure and Type 2 Diabetes: MicroRNAs as Mechanistic Links? *Current Diabetes Reports*, **17**, Article No. 18. <https://doi.org/10.1007/s11892-017-0845-8>
- [20] Gansukh, E., Mya, K.K., Jung, M., Keum, Y.S., Kim, D.H. and Saini, R.K. (2019) Lutein Derived from Marigold (*Tagetes erecta*) Petals Triggers ROS Generation and Activates Bax and Caspase-3 Mediated Apoptosis of Human Cervical Carcinoma (HeLa) Cells. *Food and Chemical Toxicology*, **127**, 11-18. <https://doi.org/10.1016/j.fct.2019.02.037>
- [21] Kodyan, J. and Amber, K.T. (2015) A Review of the Use of Topical Calendula in the Prevention and Treatment of Radiotherapy-Induced Skin Reactions. *Antioxidants (Basel)*, **4**, 293-303. <https://doi.org/10.3390/antiox4020293>
- [22] Zhang, S. (2023) Recent Advances of Polyphenol Oxidases in Plants. *Molecules*, **28**, Article No. 2158. <https://doi.org/10.3390/molecules28052158>
- [23] Weiss-Sadan, T., Ge, M., Hayashi, M., Gohar, M., Yao, C.H., De Groot, A., *et al.* (2023) NRF2 Activation Induces NADH-Reductive Stress, Providing a Metabolic Vulnerability in Lung Cancer. *Cell Metabolism*, **35**, 487-503.E7. <https://doi.org/10.1016/j.cmet.2023.01.012>
- [24] Liao, X., Zhang, Z., Ming, M., Zhong, S., Chen, J. and Huang, Y. (2023) Imperatorin Exerts Antioxidant Effects in Vascular Dementia via the Nrf2 Signaling Pathway. *Scientific Reports*, **13**, Article No. 5595. <https://doi.org/10.1038/s41598-022-21298-x>
- [25] Duan, J., Zhao, Y., Pei, F., Deng, W., He, L., Rao, C., Zhai, Y. and Zhang, C. (2023) Swietenine Inhibited Oxidative Stress through AKT/Nrf2/HO-1 Signal Pathways and the Liver-Protective Effect in T2DM Mice: *In Vivo* and *in Vitro* Study. *Environmental Toxicology*, **38**, 1292-1304. <https://doi.org/10.1002/tox.23764>
- [26] Baumel-Alterzon, S., Katz, L.S., Brill, G., Garcia-Ocana, A. and Scott, D.K. (2021) Nrf2: the Master and Captain of Beta Cell Fate. *Trends in Endocrinology & Metabolism*, **32**, 7-19. <https://doi.org/10.1016/j.tem.2020.11.002>



- [27] Zheng, D., Liu, Z., Zhou, Y., Hou, N., Yan, W., Qin, Y., Ye, Q., Cheng, X., Xiao, Q., Bao, Y., Luo, J. and Wu, X. (2020) Urolithin B, a Gut Microbiota Metabolite, Protects against Myocardial Ischemia/Reperfusion Injury via P62/Keap1/Nrf2 Signaling Pathway. *Pharmacological Research*, **153**, Article ID: 104655. <https://doi.org/10.1016/j.phrs.2020.104655>
- [28] Zhou, Z.D., Xie, S.P., Saw, W.T., Ho, P., Wang, H., Lei, Z., Yi, Z. and Tan, E.K. (2019) The Therapeutic Implications of Tea Polyphenols against Dopamine (DA) Neuron Degeneration in Parkinson's Disease (PD). *Cells*, **8**, Article No. 911. <https://doi.org/10.3390/cells8080911>
- [29] Dodson, M., Chen, J., Shakya, A., Anandhan, A. and Zhang, D.D. (2023) The Dark Side of NRF2 in Arsenic Carcinogenesis. *Advances in Pharmacology*, **96**, 47-69. <https://doi.org/10.1016/bs.apha.2022.08.002>
- [30] Yang, X., Weber, A.A., Mennillo, E., Paszek, M., Wong, S., *et al.* (2023) Oral Arsenic Administration to Humanized UDP-Glucuronosyltransferase 1 Neonatal Mice Induces UGT1A1 through a Dependence on Nrf2 and PXR. *Journal of Biological Chemistry*, **299**, Article ID: 102955. <https://doi.org/10.1016/j.jbc.2023.102955>